

Analysis of Satellite Drag

The use of thermospheric density models for calculation of the drag force on satellites is evaluated. These models are essential for precision orbit determination and for geophysical research. Drag data plays an important role in understanding the thermosphere and can contribute in a unique way to the monitoring of the next solar cycle. Nevertheless, determining the atmospheric drag on a satellite presents several problems. The current suite of thermospheric models is described and a subset of these models is analyzed quantitatively. These models are evaluated by using precision tracking data on three spherical satellites. At the lowest altitude, 270 km, all models performed equally well, but at the higher altitudes, the models did not all perform as well. The tracking data also permits an evaluation of the atmospheric indexes currently used in thermospheric models, and of the precipitation index, which is not yet included in the models. Significant correlation is found between the data and the precipitation index.

Atmospheric drag affects all satellites — in all altitude regimes — from low altitudes to beyond geosynchronous altitudes. And atmospheric drag is the largest source of error in modeling the force on many of these satellites. Through the use of good models, however, the effect of atmospheric drag on satellites can be calculated.

The primary uses of drag models are for precision orbit determination, mass determination or weighing of satellites, and investigation of geophysical phenomena. The first two applications, precision orbit determination and weighing of satellites, are considered time-critical; results must be available within hours to be useful. Geophysical investigations, however, which include atmospheric physics, are less time-critical. An *a posteriori* analysis can be used to obtain an optimal estimate of the orbit. Table 1 summarizes the applications of atmospheric drag models and the areas in satellite tracking that require drag measurements.

Satellite tracking provides an excellent vantage point for the study of atmospheric drag. The data analysis presented in this paper comes from precision radar tracking data beginning in 1985 on two spherical satellites, and from laser ranging data taken in 1986 on a third spherical satellite. The satellites have perigee heights of

270 km, 780 km, and 1,500 km. The data were used to evaluate the following thermospheric density models: CIRA 1972 [1], Jacchia 1977 [2], DTM [3], and MSIS83 [4]. Cook's [5] definition of the ballistic coefficient, C_d , was used in this analysis.

Figure 1 illustrates several aspects of the atmospheric drag problem. The drag force is a product of four factors: C_d ; the area-to-mass ratio, A/M ; the atmospheric density, ρ ; and the speed of the satellite with respect to the atmosphere, V_s . Each of these quantities will be discussed in this paper, but note now that none of these terms are known precisely. An error made in the calculation of atmospheric drag can be due to an error made in determining any of these factors, and is more than likely due to a combination of errors in all of them.

A second aspect of the atmospheric drag problem is indicated by the two separate terms for density that are listed directly below the drag-force equation in Fig. 1. Two terms are used because none of the standard atmospheric models predict reliable densities above 2,000 km, even though drag effects are observed above this altitude. The reason is that, until recently, the primary interest in drag has been in the low-altitude regime. All data used in building the atmospheric models comes from regions below 1,000 km; additional data are needed above

Table 1. Uses of Drag Models

Precision Orbit Determination (Time-Critical)

- Catalog Maintenance
- SOI
- Prediction/Forecasting
- ASAT Targeting/Threat Analysis
- Data Screening and Calibration
- Collision Avoidance
- Navigation Satellites (eg, Transit)

Weighing of Satellites (Time-Critical)

- SOI
- Damage Assessment
- Decoying of Space Assets
- Space Debris Characterization

Geophysical Investigations

- Atmospheric Physics
 - Model Development
 - Calibration of Other Thermosphere Sensors
 - Synthesis with Other Data
- Other Investigations
 - Polar Motion and Earth Rotation
 - Scientific Satellites Precision Orbits (eg, MAGSAT, SEASAT, GEOSAT, TOPEX, ERS)

1,000 km. Also, it is probable that different physical processes apply to the two regions (above and below 2,000 km).

In our analysis we use an integrated atmospheric density model. Below 2,000 km, the atmospheric density is determined from one of the previously mentioned thermospheric models, which uses such inputs as the geomagnetic index, K_p , and the F10.7-cm flux. The F10.7-cm flux is the solar flux of radiation at 2,800 MHz; this flux is assumed to scale with the flux of extreme ultraviolet radiation (which drives the thermosphere, but can't be measured from the earth's surface). We also assume that the lower atmosphere is corotating with the solid earth. Above 2,000 km, an empirically determined density fixed in inertial space is used.

The size of the drag effect is shown by a simplified model calculation in Fig. 1. All satellites are assumed to be spheres with the same A/M , which is chosen to be $0.1 \text{ cm}^2/\text{g}$, a typical value for satellite payloads. We calculate

the time for drag to change the satellite position by 12 km. This is, in a sense, the orbital error caused by ignoring drag altogether. For satellite COSMOS1179, which is a calibration sphere with perigee at about 300 km, the error (along track) is 12 km after 0.92 days, or 13.6 revolutions. For LCS4, another calibration sphere with perigee at about 800 km, there will be a 12-km error after 22.8 days, or 323 revolutions, and for LCS1, a calibration sphere with perigee at 2,800 km, the error is 12 km after 38.9 days, or 386 revolutions. Clearly, though the drag effect is far more noticeable at lower altitudes, significant drag is observed at all altitudes.

Precision Orbit Determination

The main use of drag models is for the determination of precision orbits. Because atmospheric drag is one of the largest forces on a satellite, obtaining precision orbits requires accurate modeling of the atmosphere.

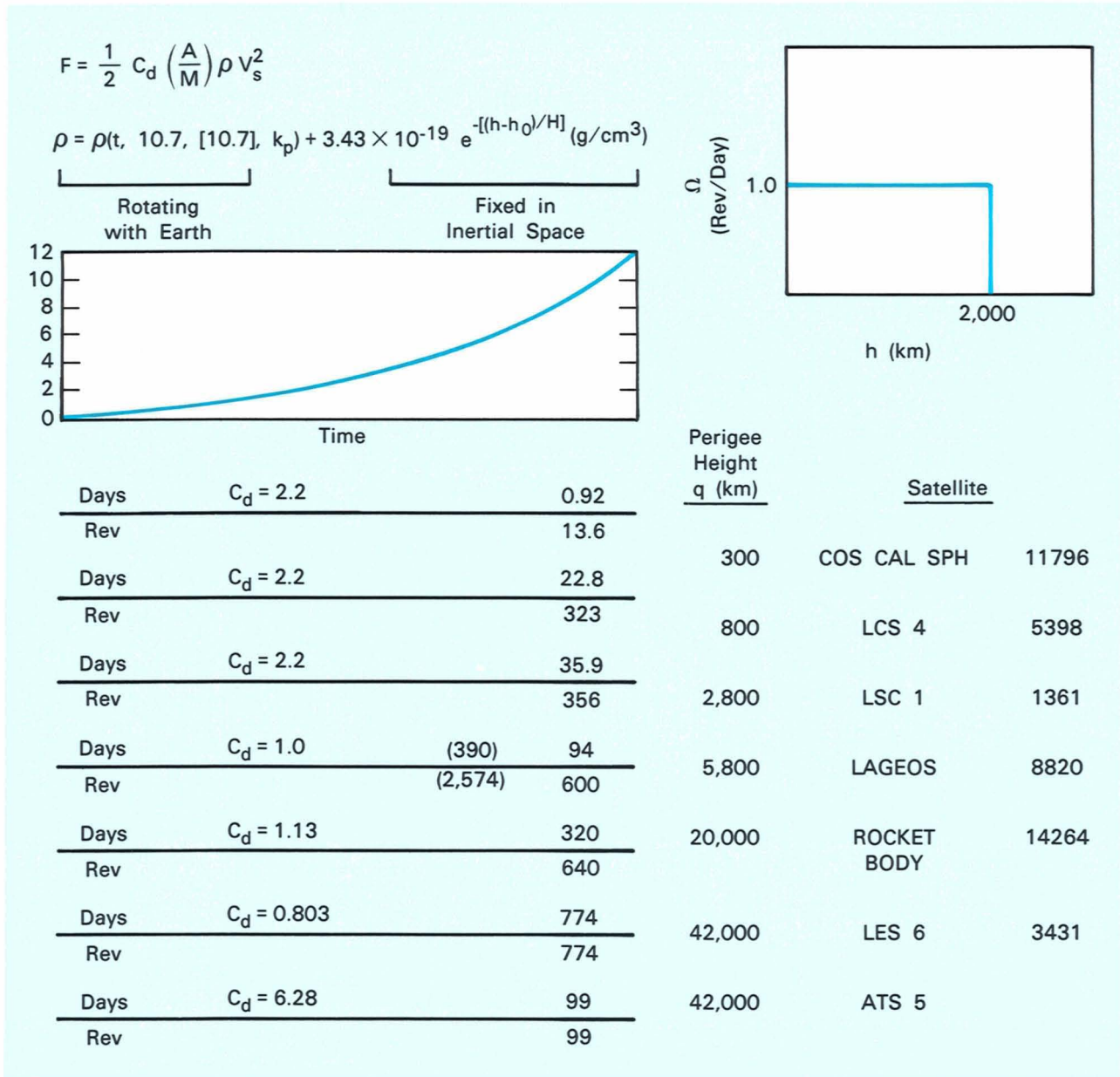


Fig. 1 — Drag effect for $(A/M) = 0.1 \text{ cm}^2/\text{g}$.

The ability to know precise satellite positions contributes to a variety of areas in satellite tracking. For example, precision orbits on satellites are needed for catalog maintenance, satellite orbit identification (SOI), collision avoidance, satellite navigation (eg, Transit), antisatellite (ASAT) targeting and threat analysis, and data screening and calibration.

Catalog maintenance depends on knowledge of a satellite's orbital elements to within a given accuracy. For data of a given quality, the best dynamical model of the orbit gives the most accurate element set for a satellite (a satellite's position and velocity). This orbital model necessarily includes the best model of atmospheric drag. By maintaining an

accurate catalog, one has available precision element sets for each satellite. A critical use of these element sets is SOI. Reliable and accurate orbits provide the most commonly used technique for the identification of satellites.

Precision elements are essential for predicting and forecasting satellite orbits. Prediction is needed for such applications as acquiring more tracking data from a pencil-beam radar, or determining when an orbit will decay, a requirement that stresses the use of atmospheric models at low altitude. Predictions are also necessary for the maneuver planning and execution needed for orbit maintenance. Furthermore, highly accurate and timely predictions of satellite position are required to target a given volume (ASAT targeting), or to assess the threat to an asset of another vehicle (threat analysis). And orbit predictions play an important role in testing new surveillance systems. New systems, such as the space-based radar and the visible optical satellite-tracking system — both currently under development — need real-time precision predictions of position, up to 24 hours in advance, to interpret sensor data properly.

Operational satellites also depend on atmospheric drag analysis for accurate predictions. The Navy Transit Navigation satellites, for example, are limited by the accuracy of drag models. Currently, there are several surface-force-compensated, drag-free, Transit satellites flown at great expense to overcome the drag problem. Better drag models would alleviate the drag issues in a fundamental way.

Atmospheric models also play an important role in the calibration of satellite-tracking data. To have confidence in inferences based on tracking data, it must have been validated, screened, and calibrated. This is an ongoing data analysis function that requires reliable and accurate orbit computation. Calibration computations are no more accurate than the precision of the orbit, which, in low altitudes, is limited by the estimation of the drag force.

A final application for precision orbits is collision avoidance. A growing population of cataloged objects in space, almost 7,000 in low

altitude, means that the possibility of collision, though small, is nevertheless real. Despite the low probability, the cost of the collision of a satellite, or even worse, of debris, with a foreign asset is so high that every step must be taken to prevent such an occurrence. Precise and timely monitoring, *ie*, maintenance of the catalog, is the only way to accomplish this task.

Mass Determination

The effects of all nongravitational forces, *eg*, drag and radiation pressure, are proportional to A/M . Therefore A/M can be found from an observed change in satellite orbit. If the size (A) of a satellite is known, say from radar cross section (RCS) observations, then the drag force can be used to determine the mass (M) of a satellite. In fact, this process has been performed more or less accurately for some years; it hinges on knowing the density and the C_d contribution to the drag-force equation. Therefore, it requires accurate assessment of the atmospheric density.

The determination of a satellite's mass and size has important implications for SOI. The combination of information about a satellite's mass and size (and perhaps its shape, attitude, and spin rate) is a second discrimination tool for SOI, perhaps as powerful as the information contained in the element sets. By monitoring this information, a change in either the orbit or the operational status of a satellite can be observed. Such changes can indicate, for example, possible damage due to a collision or an ASAT attack.

Another use of weighing satellites is for decoying space assets. The decoy problem is usually viewed in terms of replicating the size, RCS, and optical characteristics of an asset. However, the ability to weigh objects means that the mass would also have to be replicated in order to be credible. Because the cost of space objects depends on the mass in orbit, such a requirement sharply reduces the attractiveness of decoying. Issues such as response time and accuracy become paramount, of course, since decoy strategies are manifold.

Weighing satellites can also be used in the low-

altitude regime, where there is considerable debris. The debris population is continually changing as it is depleted by atmospheric drag and replenished by a variety of sources, including breakups and new rocket launches. An organized observation and analysis program is required to assess properly the population statistics and thus the hazard presented by debris. A critical element of space debris characterization is the measurement of each particle's mass, which is feasible with a good drag model and accurate tracking data.

Geophysical Investigations

Drag models used for operational tracking can provide significant insights into the fundamental physics of the thermosphere. Excellent models have been derived from analysis of tracking data. Such tracking data can also provide basic information for testing models. For example, drag data can be used to assess the models' performance and to determine basic constants within models. Drag data can also be used to calibrate other atmospheric sensors, such as instrumented satellites. Over the long term, we hope to develop a complete thermospheric model, based on physical principles, that combines observations of constituents from satellite instruments with total density obtained from analysis of satellite drag.

Other geophysical investigations depend on precision orbit computation. Currently, there are low-altitude satellites that measure the earth's geopotential, its motion in space, its polar motion, and its rotation rate. Atmospheric drag is a significant error source in the analysis of these low-altitude satellites. In addition, several low-altitude geophysical sensors (eg, MAGSAT, SEASAT, GEOSAT, TOPEX, ERS) need to know the position of a satellite at the time of measurement. Again, improvement in drag modeling will directly improve the analysis of this type of geophysical data.

Outline of Drag Problems

The satellite-tracking community is mainly interested in the determination of the

atmospheric drag force. The calculation of neutral density from thermospheric models is only one piece of the problem; a number of other issues have to be addressed to achieve the desired capabilities.

As shown in Fig. 1, the drag force per unit mass on a satellite, which is the measured force, is

$$F = \frac{1}{2} C_d \left(\frac{A}{M} \right) \rho V_s^2 \quad (1)$$

where C_d is the ballistic coefficient, A/M the area-to-mass ratio, ρ is the atmospheric density, and V_s is the speed of the satellite with respect to the atmosphere. V_s is the vector sum of the speed of the satellite, V_{sat} , and the speed of the atmosphere, V_{atms} (wind speed). In our analysis, we assume that the lower atmosphere corotates with the earth.

One of the main problems in determining the drag on a satellite is that none of the quantities in Eq. 1 are known exactly. Consider the definition of C_d , given in Fig. 2. C_d , which must be determined for each satellite, depends on the type of scattering that takes place between the surface of the satellite and the neutral particles in the atmosphere. But there are fundamental unknowns in the physics of scattering. For example, we cannot reliably predict how particles in free molecular flow scatter from a surface in space, nor do we know how that surface and the scattering change after long exposure in space.

A theory of scattering is summarized in Fig. 2. Verification of the theory is needed, along with determination of several constants. Figure 2 gives the mathematical formalism for solar radiation pressure, neutral drag, and charge drag, three effects that share common elements. It is, therefore, instructive to consider them together. In all three cases, the force on a general surface element depends on the scattering mechanism and on the flux of photons, neutral particles, or charged particles.

Two scattering mechanisms are indicated: specular scattering and a Lambert's law "diffuse" scattering. These two are considered to be the limiting cases, one in which the scatterer completely "remembers" the information about

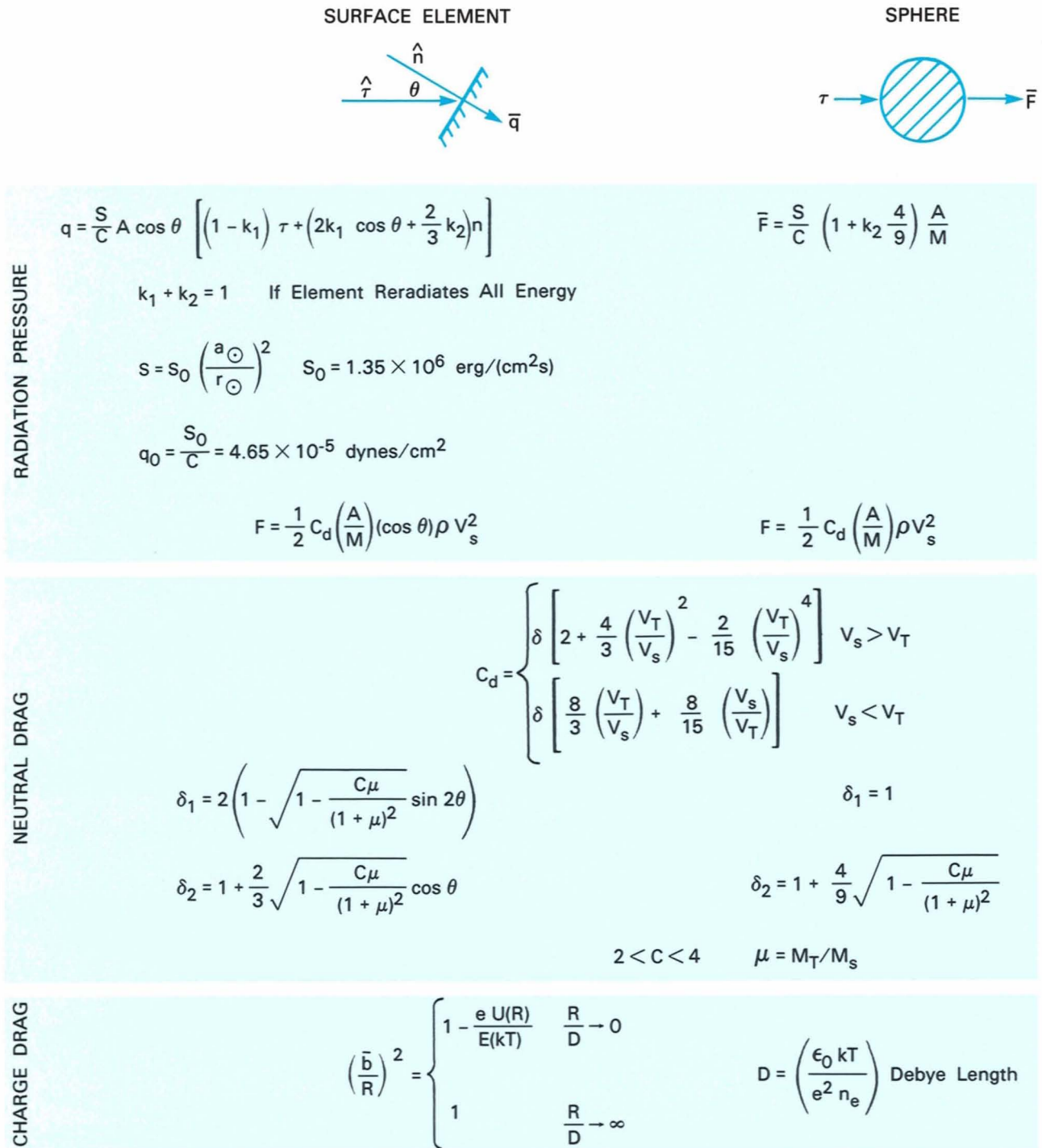


Fig. 2 — Mathematical formalism — nongravitational forces.

the incoming flux vector-momentum (specular), and the other in which no information is "remembered" (diffuse). Other scattering mechanisms are also possible; in general,

surfaces do not behave completely as specular or diffuse. A better model would be to assume a fractional part of both the diffuse and specular components on the satellite surface.

For neutral drag, the scattering interaction depends on the surface material of the satellite, and on the molecular weight and temperature, or thermal velocity (V_T), of each particle. The thermal dependence is theoretically modeled in terms of the ballistic coefficient. The molecular weight of the atmospheric constituent and of the surface material of the satellite are modeled through an accommodation factor, δ (δ_1 for specular scattering and δ_2 for diffuse scattering). However, even if the chemical constituents of the atmosphere are known (using laboratory measurements [6]), the value of C_d can not be determined to better than 5% [7].

The projected cross section in Eq. 1, A , also must be determined for the majority of satellites. In general, the cross section depends on a satellite's aspect angle, which is often difficult to calculate and probably has to be observed. In our study we determined the atmospheric drag on selected spherical satellites so that questions of aspect did not arise. To calculate A/M in Eq. 1, the true mass must also be known. This value is essential if drag measurements are to be used to predict absolute density.

The next term in Eq. 1 is ρ , the atmospheric density. This value is usually predicted by thermospheric models, although the models themselves do not predict the density to better than 15% at low altitudes (less than 300 km). The model prediction becomes worse with increasing altitude.

The last term in Eq. 1 is the speed of a satellite with respect to the atmosphere. The speed of a satellite with respect to the earth is known with fairly high precision. However, V_s also depends on the speed of atmospheric winds. Satellite experiments, drag analysis, and theoretical models show that there are significant winds and gravity waves in the thermosphere. Since these winds can have speeds of several hundred meters per second, a speed that is comparable to satellite velocities, any advance in modeling of satellite drag must therefore include information about winds.

Abundant evidence shows that atmospheric drag affects all satellites, even though the effect may be small at high altitudes. For space surveillance, high-altitude drag is not as serious

as low-altitude drag; the cumulative effects take months to be operationally significant. Yet the existence of this drag, not predicted by any of the current models, indicates a flaw in our understanding of the thermosphere. We cannot accept a model as comprehensive if it does not satisfactorily explain all observed atmospheric phenomena.

Further difficulties in determining atmospheric drag are caused by the geophysical inputs to drag models. In the previous section we identified a number of uses that are time-critical, *ie*, that need results within hours to be useful. Most of the present suite of models use geophysical parameters such as F10.7 and K_p as measures of energy input to the atmosphere. These are surrogate parameters to begin with, since direct measurements of the ionospheric current and the solar extreme ultraviolet (EUV) flux are not available. The indexes that are used have certain inherent problems. The K_p and A_p are planetary indexes and so cannot represent localized disturbances. (K_p and A_p are both measures of the geomagnetic index; they are monotonically related by a nonlinear function.) The F10.7-cm flux, on the other hand, can represent the EUV solar flux, although it, in itself, has no direct influence on the atmosphere. The models also assume that we use data obtained after careful calibration and reduction by the geophysical service operated jointly by NOAA (National Oceanic and Atmospheric Administration) and the USAF. Generally, the final data values are available only after some weeks or months and are not available for time-critical missions. We must, therefore, use predictions of these values based on incomplete information.

Table 2 summarizes the problems associated with determining atmospheric drag.

Present Drag Models

Thermospheric density models for heights above 120 km have been derived from the analysis of satellite drag since the launch of Sputnik I. Satellite drag measures only total density and contains no direct information about satellite composition. Early models

identified the fundamental dependence of the upper atmosphere on solar flux; geomagnetic index; and diurnal, monthly, and seasonal variations. Atmospheric models based on satellite drag data are typified by the COSPAR International Reference Atmosphere of 1972 (CIRA72), which is based on the Jacchia 1971 model [1], and by the DTM 1978 model [3].

Atmospheric composition can be inferred or measured using both ground-based incoherent backscatter radar measurements and satellites instrumented with mass spectrometers and accelerometers. This type of data has been used to construct the so-called mass spectrometer and incoherent backscatter (MSIS) models [4, 8, 9].

Jacchia attempted to merge drag and composition data into a combined model: Jacchia 1977 [2]. The Jacchia 1977 model has two modifications: a 1977 addendum, and a revision [10]. An additional version of the Jacchia 1977 model, known as the Jacchia-Bass model [11, 12], was developed at the Air Force Geophysical Laboratory.

These models are all relatively simple. They can be characterized as static diffusion models that only incorporate dynamics implicitly. The processes are, as yet, too complex to formulate a model based on physical principles alone.

The models we tested initially were the Jacchia 1977 and the MSIS83 models. We also tested the

Table 3. Seven Density Models Tested

J71	= Jacchia 71, aka CIRA 1972
DTM	= Barlier <i>et al.</i> , 1978
MSIS83	= Hedin, 1983
J77	= Jacchia 77, as defined in SAO SR 375
J77'	= Jacchia 77 + analytical approximation
J77''	= Jacchia 77 + 1981 changes in AFGL report
J77'''	= Jacchia 77 + 1981 changes + analytical approximation

Jacchia 1971 (CIRA72) model, because it is a widely used standard, and the DTM 1978 model, which was designed specifically to evaluate satellite drag. During the analysis, however, a number of issues concerning the Jacchia model arose, which required testing of several variants. At this point, the results on seven models have been assembled. The development and testing of these models led to insights into the models and the scattering mechanisms they use.

The seven models are listed in Table 3. The four versions of the Jacchia 1977 model evolved because of two revisions dealing with geomagnetic effects. The first was an analytic approximation to a geomagnetic effect described by Eq. 32 in Ref. 2. The second revision resulted from combining drag data with ESRO4 satellite data [10]. These revisions are discussed in more detail in Ref. 7. J77' includes the analytic approximation, J77'' includes the revision in Ref. 10, and J77''' includes both sets of revisions.

The J71, J77, J77', and DTM models are predominantly based on satellite drag measurements obtained in the region from 250 to 1,000 km. The J77'' and J77''' models also incorporate a considerable amount of satellite-measured composition data from the ESRO4 satellite at altitudes ranging from 250 to 800 km and less than 40 degrees in latitude. The MSIS model is completely based on satellite mass

Table 2. Summary of Problems Associated with Atmospheric Drag

Physics
Satellite Aspect
Geophysical Input:
Accuracy and Prediction
Composition, Temperature, and Density Models
Winds and Super-Rotation
Gravity Waves
High-Altitude Drag

Table 4. Timing Test of the Atmospheric Models

J71	11.10 seconds
DTM	16.22 seconds
J77	35.38 seconds
J77'	41.98 seconds
J77''	33.26 seconds
J77'''	36.70 seconds
MSIS83	116.84 seconds (86.74)

spectrometer and ground-based incoherent scatter data, the latter used primarily to measure neutral temperatures. The majority of mass spectrometer data was obtained from the Atmospheric Explorer satellites in the altitude regions from 100 to 500 km.

A timing test was performed on each of the different models. In the test, each model was called 4,000 times in a variety of positions and hour angles. The results are presented in Table 4.

The two times listed for the MSIS83 model refer to the geomagnetic A_p parameters that were used as input. The MSIS83 program has the option of using either the daily value of the A_p or an array of seven A_p indexes, including the daily A_p index and time averages of the three-hour A_p indexes. The shorter time listed for MSIS83 refers to a program run with only the daily A_p value input. From the standpoint of orbital decay, no significant difference was found between these two options. In our standard procedure, the array of A_p values as inputs to the MSIS83 model was used.

Our timing test shows that the MSIS83 model is significantly slower than any of the Jacchia models. This result contradicts the general consensus in the community, which is that the J77 model is much slower computationally than either the J71 model or the MSIS model [13, 14]. We assume that this discrepancy is caused by our implementation of the J77 model; we used a look-up table similar to that used in the J71 program. Note also that the DTM model runs faster than any the models except the J71 model.

We ran a computer simulation comparing the

ratios of the densities predicted by the Jacchia 71, J77, J77', J77'', and MSIS83 models to those predicted by the J77'' model for the 300-km altitude. This simulation was performed to see how the models differ. The J77'' model was selected as the standard model because it was found to be the best overall model in predicting satellite drag for our data set. All hour angles were sampled with latitude coverage between +60 and -60 degrees. The daily and average solar flux values were set at 74 (a low solar flux condition), and a Julian date of 46144 was used. The results for two different K_p values corresponding to a typical mean K_p value ($K_p = 2.5$) and to a high K_p value ($K_p = 5.0$) are presented in Table 5. In each case, 2,500 data values were averaged.

The results show that at 300 km the models are all in reasonable agreement. A 15% difference between the mean ratios of the models is apparent. Although it is known that atmospheric models cannot predict densities to better than 15% (a number that increases at higher altitudes), we would like a 5% prediction capability of drag, and aim for a 1% capability.

We have found that the J77, J77', and J77''' are clearly inferior to the J77'' in all cases [7]. These models were not evaluated further.

Measurements of Satellite Drag

The rest of this paper investigates measurements of satellite drag and suggests improvements that can be implemented in future drag models. In particular, we describe the measurements we made of atmospheric drag and how we used the measurements to evaluate the atmospheric models. We also used these measurements to evaluate different atmospheric indexes, including those currently used as inputs and a new index that is not yet being used by the models.

Measurements of satellite drag were acquired by taking daily tracks of spherical satellites from Lincoln Laboratory and NASA facilities. Lincoln Laboratory operates two satellite-tracking radars that provide data with an accuracy of 1 m [15-17]. One of these systems is the Altair radar on the Kwajalein Atoll (Marshall Islands); the

Table 5. Comparison of Densities Derived by the Various Atmospheric Models to the J77" Model at 300 km

		$K_p = 2.5$		$K_p = 5.0$	
		Mean Ratio (Model/J77")	Standard Deviaton (%)	Mean Ratio (Model/J77")	Standard Deviation (%)
1.	Jacchia 71	1.082	6.5	1.16	9.1
2.	Jacchia 77				
	J77	0.886	6.3	0.81	8.7
	J77'	0.872	7.3	0.81	9.4
	J77"	1.000	0.0	1.00	0.0
	J77'''	0.880	8.4	0.78	14.3
3.	DTM78	0.867	5.3	0.81	5.1
4.	MSIS83	0.934	9.3	0.93	10.2

other is the Millstone L-band radar in Westford, MA. NASA operates a network of laser-ranging stations that provide data on satellites equipped with cube corner reflectors. The accuracy of these data is better than 2 cm [18].

For two satellites, LCS4 and COSMOS1179, daily tracks have been taken since the beginning of 1985. Daily tracks on the third satellite, EGS (also known as Agasii), have been taken since launch in 1986. Data from all of 1985 have been analyzed for the former satellites, as well as the initial two months of data on EGS in 1986. These satellites are described in Table 6, where the semi-major axis (a) and the perigee height (q) are given in km, A/M is given in cm^2/g , and the inclination (I) in degrees. The eccentricity is e .

The orbit computation program DYNAMO uses an iterative least-squares procedure to fit the data. The program begins with an initial or reference state that is differentially corrected

until convergence. Figure 3 shows this procedure. In addition to a model for atmospheric drag, DYNAMO uses a full geopotential model [20], plus models for lunar and solar perturbations (ephemeris in the J2000 system [19]), body and ocean tides [21], solar radiation pressure, earth-reflected albedo pressure, and general relativity.

Atmospheric density models were used in the orbit computation of these data sets to calculate atmospheric drag. When used, these models include the final F10.7-cm solar flux and geomagnetic index K_p data [22]. A scale parameter (S) is also introduced in the least-squares orbit determination program.

S is a least-squares-fit parameter that is used for each orbital arc and that scales the entire drag model. It can be interpreted as an indication of the adequacy of the drag, and thus of the thermospheric model used to compute the

Table 6. Satellites Used for Evaluation of Density Models

Cospar #	NSSC#	Name	$a(\text{km})$	e	$I(^{\circ})$	$q(\text{km})$	A/M
1980 37 A	11796	COSMOS1179	7,028	0.051	82.9	270	0.038
1971 67 E	5398	LCS4	7,207	0.008	87.6	780	0.285
1986 61 A	16908	EGS	7,878	0.001	50.1	1,500	0.045

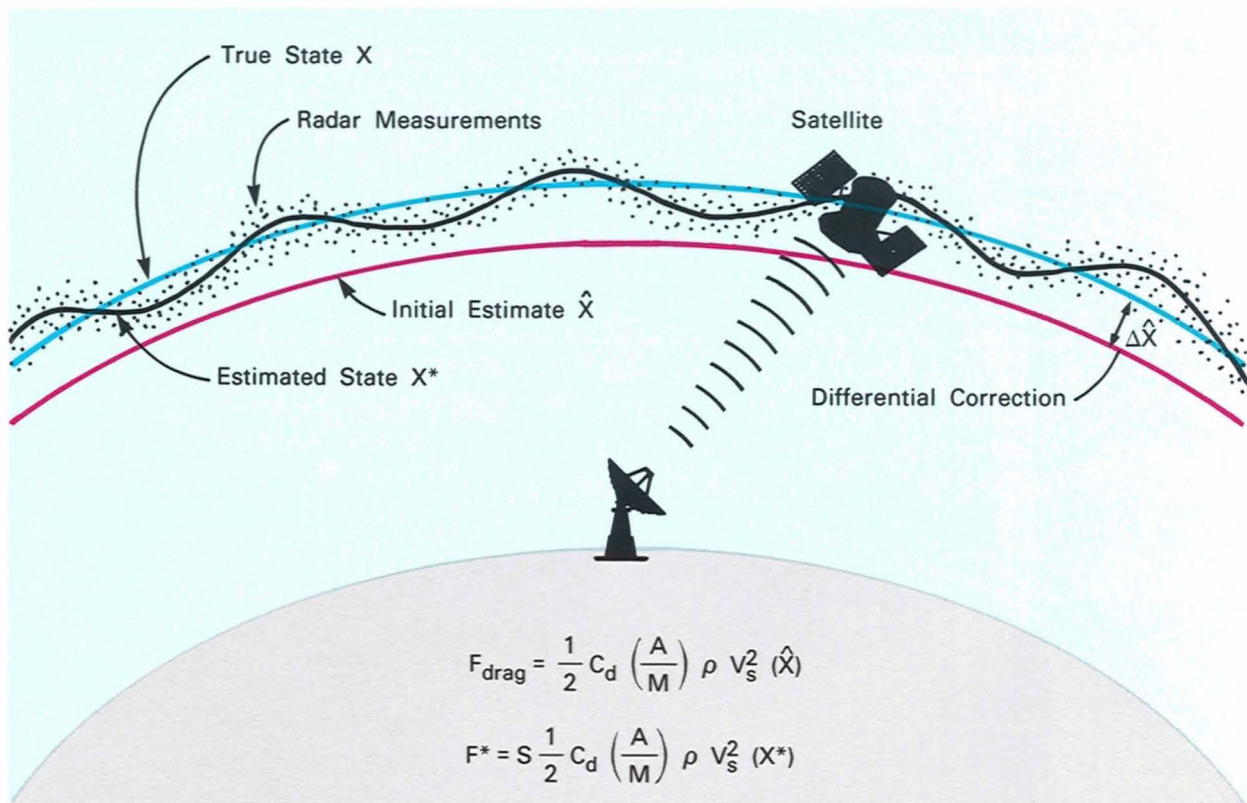


Fig. 3 — Orbit determination procedure.



F_{drag} is the Along-Track Drag Force per Unit Mass Acting on a Satellite

$$F_{\text{drag}}^* = \frac{1}{2} C_d \left(\frac{A}{M} \right) \rho V_s^2 \xrightarrow{\text{Used In}} X^* \text{ Reference State}$$

$$F_{\text{drag}} = S \left[\frac{1}{2} C_d \left(\frac{A}{M} \right) \rho V_s^2 \right] \xrightarrow{\text{Used In}} X \text{ Estimated State}$$

C_d = Ballistic Coefficient — Known for Most Spheres

$\frac{A}{M}$ = Area-to-Mass Ratio of Satellite — Known for Most Spheres

V_s = Satellite Velocity Known

ρ = Atmospheric Drag

Fig. 4 — Estimation of drag force.

drag. If S is less than unity, then the atmospheric density predicted by the model is too large; if S is greater than unity, then the atmospheric density predicted by the model is too small. See Fig. 4 for further clarification of S .

With a complete force model, and the scale factor, the orbital arcs do generally fit within the accuracy of the data (several meters). The orbital arcs are computed with one-day spacing, using between two and four days of data; any given pass of data will be in at least two orbit fits. This procedure is used for data validation, as well as for checking orbital consistency. The computed scale factors can be plotted as a function of epoch and the plots used to give an indication of how the density model involved in the drag calculation may be deficient. Figure 5 is an example of the scale-factor data for COSMOS1179 and for the J77"

model over a year's time.

Scale factors were computed for each satellite and for each atmospheric model. In addition, scale factors were computed for both the specular- and diffuse-scattering case. These data are summarized in Table 7. The first term under each satellite is the average scale factor, S , for that data set; the second term is the standard deviation, σ .

The results for each satellite will now be discussed.

COSMOS1179

COSMOS1179 (COSMOS Series #1179) is known to be a sphere. Its mass, however, is not known from independent information. Therefore, an A/M ratio based on an average drag has been adopted. Because of the use of

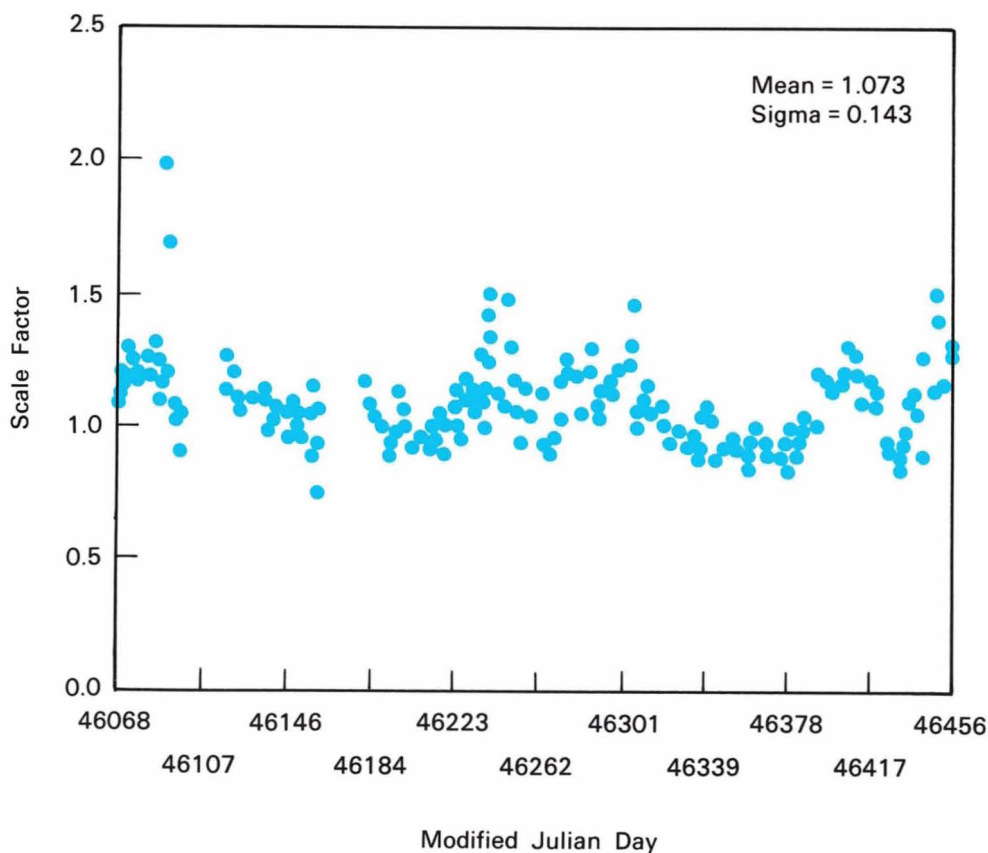


Fig. 5 — Jacchia 77" diffuse scale for COSMOS1179.

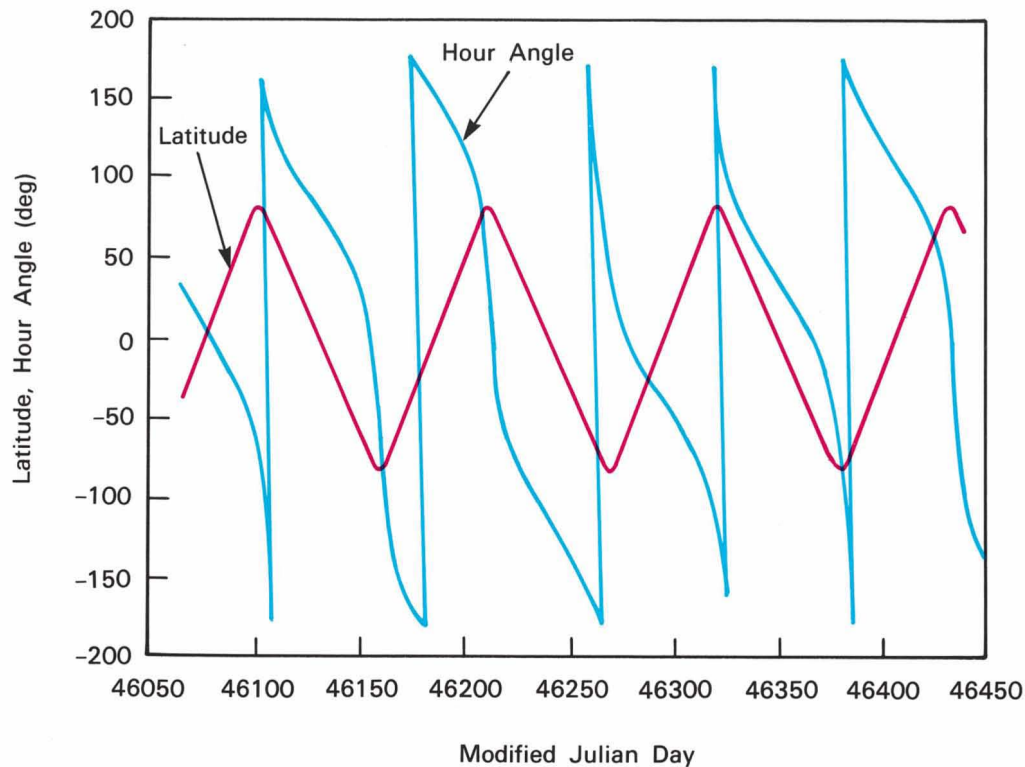


Fig. 6 — Latitude and hour angle for COSMOS1179.

this assumption, COSMOS1179 can only be used for a relative assessment of atmospheric models. The scale factors for J77" were computed assuming a diffuse-scattering mechanism and are presented in Fig. 5.

Throughout the time period analyzed, the eccentricity of COSMOS1179 has been large enough that drag occurs mainly at perigee, where the scale height is about 7 km. Therefore, the orbit only samples the density at one geographic point per revolution. Figure 6 gives the latitude and solar hour angle of the perigee point for the interval analyzed. Both latitude and hour angle are completely sampled, and there is no simple correlation with the variation in S seen in Fig. 5.

These factors were computed for the satellite using the assumption of specular scattering. The mean values of the scale factors for the two cases are fairly similar, as can be seen in Table 7. From the theoretical standpoint, a significant difference is not expected between the specular

and diffuse cases, because the drag at 295 km is primarily from oxygen and nitrogen. The mean molecular weight is approximately 16, which results in a value for the accommodation coefficient, the term used in the model for diffuse scattering, of nearly 1. An accommodation coefficient of 1 results in the same value of C_d as that predicted by the model for specular scattering. The scale factors for the specular scattering are not significantly different.

As mentioned, the absolute mean scale factors are not significant in this satellite. However, the fact that the scale factors differ by at most 5% indicates that all the models are in good agreement. The variation about the mean is smallest for the J77" model, though all the models differ by 2% at most. On this basis one could marginally choose the J77" as the best model. This difference is not believed to be significant. All models are equally good (or bad) at 275-km altitude for all latitude, hour angle, and geophysical data.

LCS4

LCS4 (Lincoln Calibration Sphere #4), a satellite in a circular orbit at approximately 780-km altitude, was built by Lincoln Laboratory. Its physical characteristics, such as A/M and the composition of its outer surface (aluminum), are known. Because of its nearly circular orbit, the satellite does not provide a clear association of position with the effect of drag; nevertheless, the average drag can be analyzed.

At 780 km, the scale factors for the models are quite different from those found for COSMOS1179. The orbital fits have been carefully scrutinized. The observed variability in S is believed to represent real variations in the atmospheric density at 780-km altitude, which are not predicted by any of the models. In all cases, it can be seen that the scale factors are 20% to 30% less than unity, indicating that the predicted drag is too large by this factor.

At 780-km altitude, the principal atmospheric constituents are hydrogen and helium. For these constituents, the difference between specular and diffuse scattering is quite large, resulting in diffuse ballistic coefficients 20% to 30% larger than specular ones. The mean scale factors, assuming the specular-scattering mechanism, are all approximately 0.9. The general agreement among the various models persuades us that

- a) the specular-scattering model is correct for the polished aluminum spherical satellite, and
- b) there may be a systematic overestimate of the density by as much as 12%.

The J71 model has the best mean value and the DTM has the smallest variability. However, the differences may not be significant — the uncertainty in C_d may be as much as 4%.

A further issue arises because of uncertainty about LCS4. This satellite was one of two satellites fabricated by Lincoln Laboratory at the same time. Both satellites were one-square-meter radar calibration spheres made of polished aluminum, identical in all but one respect. The records show that one sphere, the "G" sphere, failed on launch and never made it to orbit. The second, the "C" sphere, became

LCS4 on launch. Both spheres were carefully measured, including the mass, which was given in the records as 38.186 kg for the "G" sphere, and 35.203 kg for the "C" sphere. Because the two spheres were unmarked and virtually indistinguishable, we cannot rule out the possibility that they were interchanged during ground handling, and that the "G" sphere actually made it to orbit as LCS4. Recent analysis of LCS4 solar radiation pressure perturbations has resulted in estimates of the mass consistent with the originally adopted "C" sphere. In this case, all the recent density models are in better agreement with the data. To account for this possibility, the scale factors can be multiplied by 1.085. Then, assuming specular reflection, the MSIS83 has a mean-scale factor of virtual unity, and the J77" is 0.95. Both values are within the uncertainty of C_d . In any event, the recent models are in acceptable average agreement at 780 km, although there are large variations in the density that are not modeled. DTM is the model with the smallest variability for LCS4.

EGS

EGS (Experimental Geodetic Satellite) is a spherical satellite in a circular orbit at 1,500-km altitude, equipped with laser cube corner reflectors. The laser ranging data, provided by NASA since launch in July 1986, has allowed the study of the density model at 1,500 km. This altitude is higher than any of the data used in constructing the models and measures how well the predicted densities of the models can be extrapolated. The EGS satellite has a known A/M , which is given in Table 7, and a surface made of aluminum with holes for the laser cube corner reflectors.

Preliminary calculations on two months of data have been performed with the MSIS83 and J77" models. The scale factors were computed for both a diffuse- and a specular-scattering mechanism. Since the atmosphere at 1,500 km is mostly hydrogen, a significant difference in the result would be expected. In Table 7, the specular-scattering assumption leads to scale factors of 1.9 and greater; the MSIS83 mean

Table 7. Summary of Scale Factors

<i>Diffuse</i>				
<i>Satellite</i>	<i>COSMOS1179</i>	<i>LCS4</i>	<i>EGS</i>	
<i>Model</i>	\bar{S}/σ	\bar{S}/σ	\bar{S}/σ	
J71			1.293/0.691	
J77"	1.106/0.146	0.715/0.321	1.389/0.617	
MSIS83	1.177/0.138	0.753/0.345	1.665/1.220	
DTM78		0.878/0.255	1.344/0.570	
<i>Specular</i>				
<i>Satellite</i>	<i>COSMOS1179</i>	<i>LCS4 "C"</i>	<i>LCS4 "G"</i>	<i>EGS</i>
<i>Model</i>	\bar{S}/σ	\bar{S}/σ	\bar{S}/σ	\bar{S}/σ
J71	1.024/0.114	1.024/0.374	1.111/0.374	
J77"	1.108/0.153	0.876/0.333	0.950/0.333	1.919/0.839
MSIS83	1.183/0.152	0.923/0.325	1.001/0.325	2.397/1.220
DTM78	1.152/0.169	1.036/0.229	1.124/0.269	

value is 2.39. The conventional diffuse-scattering model gives an average scale factor of 1.39 for the J77" and 1.67 for the MSIS83. *A priori* one would choose diffuse scattering for aluminum, and this was adopted. The analysis shows that J77" underestimates the density at 1,500 km by about 30%; MSIS83 underestimates the density by about 60%. This is consistent with the results for LCS4, where J77" was found to give larger densities than MSIS83 at the 780-km altitude.

Evaluation of Atmospheric Indexes

In addition to evaluating the atmospheric models, the derived scale factors can be used to determine how well the effects of the different indexes are being modeled and to evaluate whether a new index is of value to future modeling efforts. We did this by correlating the series of derived scale factors with different series of atmospheric indexes, including the daily F10.7-cm flux, the K_p , and the precipitation index.

The precipitation index is the only parameter we studied that is not being used as an input to any of the atmospheric models. This index

quantifies the intensity and spatial extent of high-latitude particle precipitation, based on observations made along individual passes of the NOAA/TIROS weather satellites. The satellites, which are in circular sun-synchronous orbits at 850 km [23], measure the precipitation index in near real time. We analyzed the power levels of the precipitation index.

The atmospheric parameters were averaged over the same time interval as the data used to compute the orbital arcs. For COSMOS1179, three days of data were averaged for each parameter; for LCS4, four days of data were averaged. Each series of atmospheric data was then correlated against the series of scale factors determined for both satellites, using each of the four different atmospheric models. In some cases, a single model had two series of scale-factor data — the scale factors corresponded to specular and diffuse scattering. Whether scattering was specular or diffuse did not affect the correlation of the series of atmospheric parameters against the series of scale factors.

The results for each atmospheric parameter are presented in Tables 8a, b, and c. In all cases,

the correlation coefficients were computed from scale factors and geophysical data with the average subtracted, *ie*, these data have zero mean. A correlation coefficient was determined for each atmospheric model and each satellite; a value of greater than 0.2 was considered to be significant correlation. The data discussed in Table 8 are from the first six months of data in 1985, with one exception. The bracketed value in the J77" columns for COSMOS1179 Diffuse is the data for all of 1985.

The results of the correlation between the series of daily F10.7-cm values and the series of determined scale factors are given in Table 8a. For the lower satellite, the F10.7-cm flux is modeled fairly accurately. Problems that existed in the J71 model seem to have been corrected in the later models.

The results of the correlation between the K_p indexes and the scale factors are given in Table 8b. The K_p index is used to model the influence of geomagnetic fluctuations in the atmosphere. The K_p values and the series of scale factors determined for both satellites appear to have a significant correlation.

Figure 7 shows the correlation between the K_p data and the scale factors for the Jacchia 1977 S and the MSIS83 S models. (S indicates specular scattering.) The mean of each data set has been determined and subtracted from the series. The y-axis therefore represents the data, with the mean subtracted; the x-axis represents time. These data illustrate the features in the

data sets that are correlated.

Based on the data for the lower satellite, the MSIS model shows slightly less correlation with K_p than does the Jacchia 1977 model, indicating that it better models the atmospheric response to changes in this index. We should point out that the MSIS model uses the A_p index, rather than the K_p index. We computed the correlation between the A_p index and these data sets. The results were very similar to the results presented in Table 8b. The correlation of the DTM model with K_p at 275 km is similar to the others (0.40), but at 780 km it has a significantly smaller correlation (0.09).

The results of the correlation between the precipitation power index and the scale factors are given in Table 8c. As the Table 8c shows, this index has a significant correlation with the scale factors of the atmospheric models and both satellites. Of all the parameters we investigated, the highest average correlation coefficients were seen with this index. Figure 8 illustrates in greater detail the correlation between the scale-factor data and the precipitation index. The precipitation index is not used by any of the models to predict the atmospheric response to geomagnetic activity. Based on these data, we think that the precipitation index should be included in future atmospheric models. There is significant correlation between the precipitation index and the K_p . The correlation coefficient between the K_p and precipitation data sets is 0.47; some of the correlation observed with the

Table 8a. Correlation Coefficients for F10.7 cm Flux

	COSMOS1179		LCS4	
	Specular	Diffuse	Specular	Diffuse
J71	0.18		0.35	
J77"	-0.14	-0.15 (-0.02)	-0.07	-0.01
DTM 78	0.02		0.12	0.12
MSIS83	0.04	0.06	0.11	0.02

Table 8b. Correlation Coefficients for K_p

	COSMOS1179		LCS4	
	Specular	Diffuse	Specular	Diffuse
J71	0.21		-0.24	
J77"	0.40	0.39 (0.27)	0.27	0.29
DTM	0.40		0.09	0.14
MSIS83	0.28		0.35	0.28

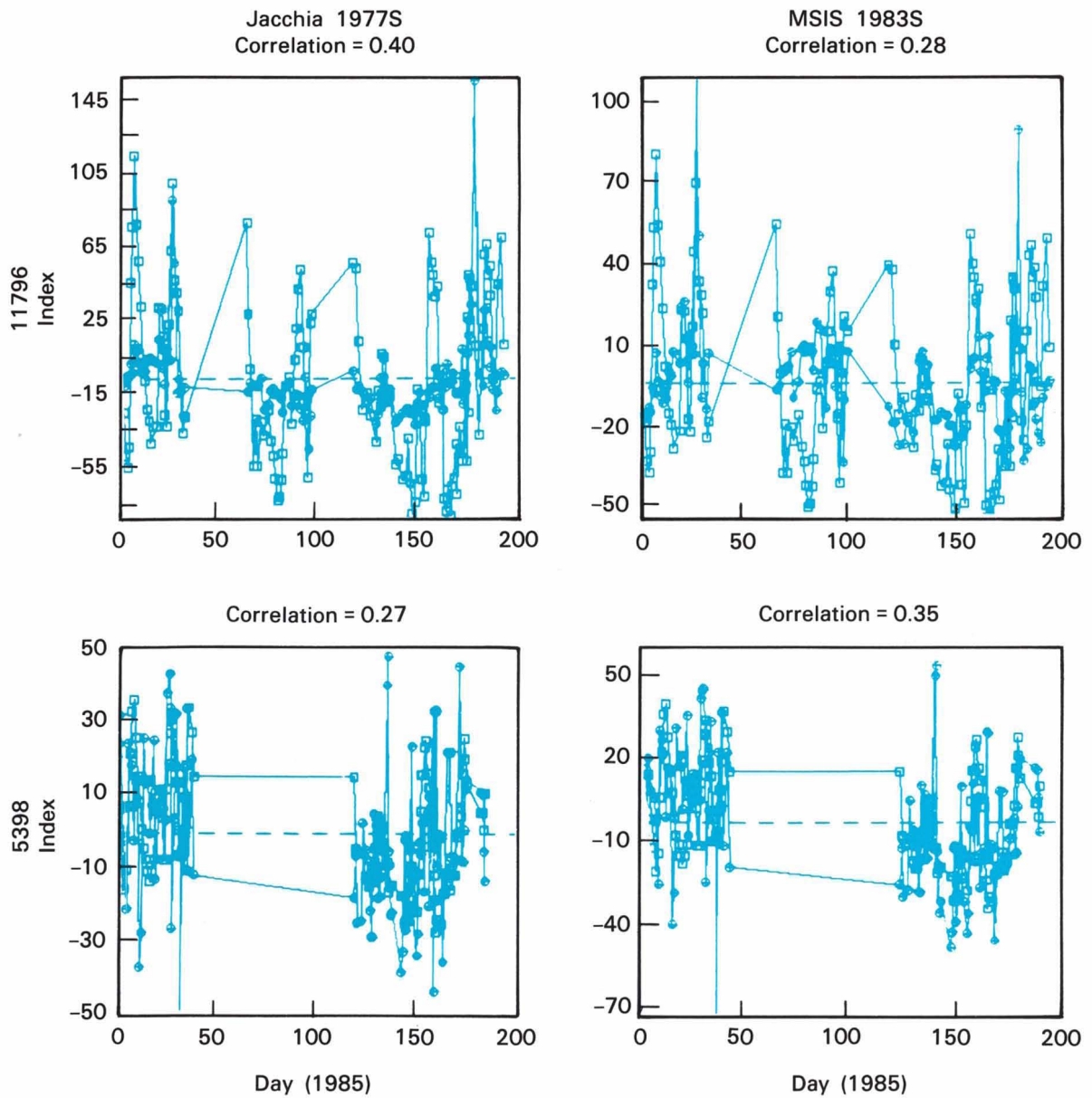


Fig. 7 — Correlation of K_p index with scale factors.

K_p could actually be leakage of the precipitation index correlation. Clearly this issue needs more data to be resolved.

Summary

We have tested atmospheric density models at 275 km, 780 km, and 1,500 km. At the two lower altitudes, all models are in good agreement — in the sense that they give the same average performance. But they all exhibit significant departures from the actual density, and it is necessary to include “solve for” parameters in orbit determination to match the tracking data.

We are continuing work in six areas:

1. Extending the data for all three satellites, to avoid any biasing due to seasonal effects, and to improve the sampling.
2. Determining the mass of COSMOS1179 and LCS4 using satellite orbit perturbations. At present it is routine to determine the mass of high-altitude satellites from perturbations due to solar radiation pressure. For lower satellites, this method has not been possible until now because the effects of geopotential model errors dominated the solution. Recent geodetic solutions show promise of changing the situation. In this case we can hope to make some statement about the absolute densities at 275-km altitude and to clarify the ambiguity about the mass of LCS4.
3. Exploring alternate indexes or variables,

such as the precipitation index, as input to the density models.

4. Expanding the source of accurate tracking data on these satellites in order to increase the space and time resolution of the drag determinations.
5. Examining the accuracy of forecasting drag for prediction of satellite orbits.
6. Obtaining data on other low-altitude satellites.

Conclusions

1. No model does an adequate job of modeling the atmospheric density.
2. There is no agreement on which model is best. We find that the differences among models, though measurable, are much less than the agreement among the models.
3. There are real physical variations in the atmosphere that are not modeled by any of the current suite of atmospheric models. New model parameters are needed (eg, winds, gravity waves) [24].
4. The inclusion of the precipitation index in future atmospheric models should be investigated. Significant correlation was observed between the precipitation index and the scale factors at 275 and 780 km.
5. Overall, these models have at most 18% difference about the mean, when averaged over all latitudes and hour angles below 800 km. However, the variance of

Table 8c. Correlation Coefficients for the Precipitation Index

	COSMOS1179		LCS4	
	Specular	Diffuse	Specular	Diffuse
J71	0.42		-0.15	
J77"	0.48	0.46 (0.37)	0.36	0.40
DTM78	0.53	0.28	0.19	
MSIS83	0.42	0.42	0.45	0.36

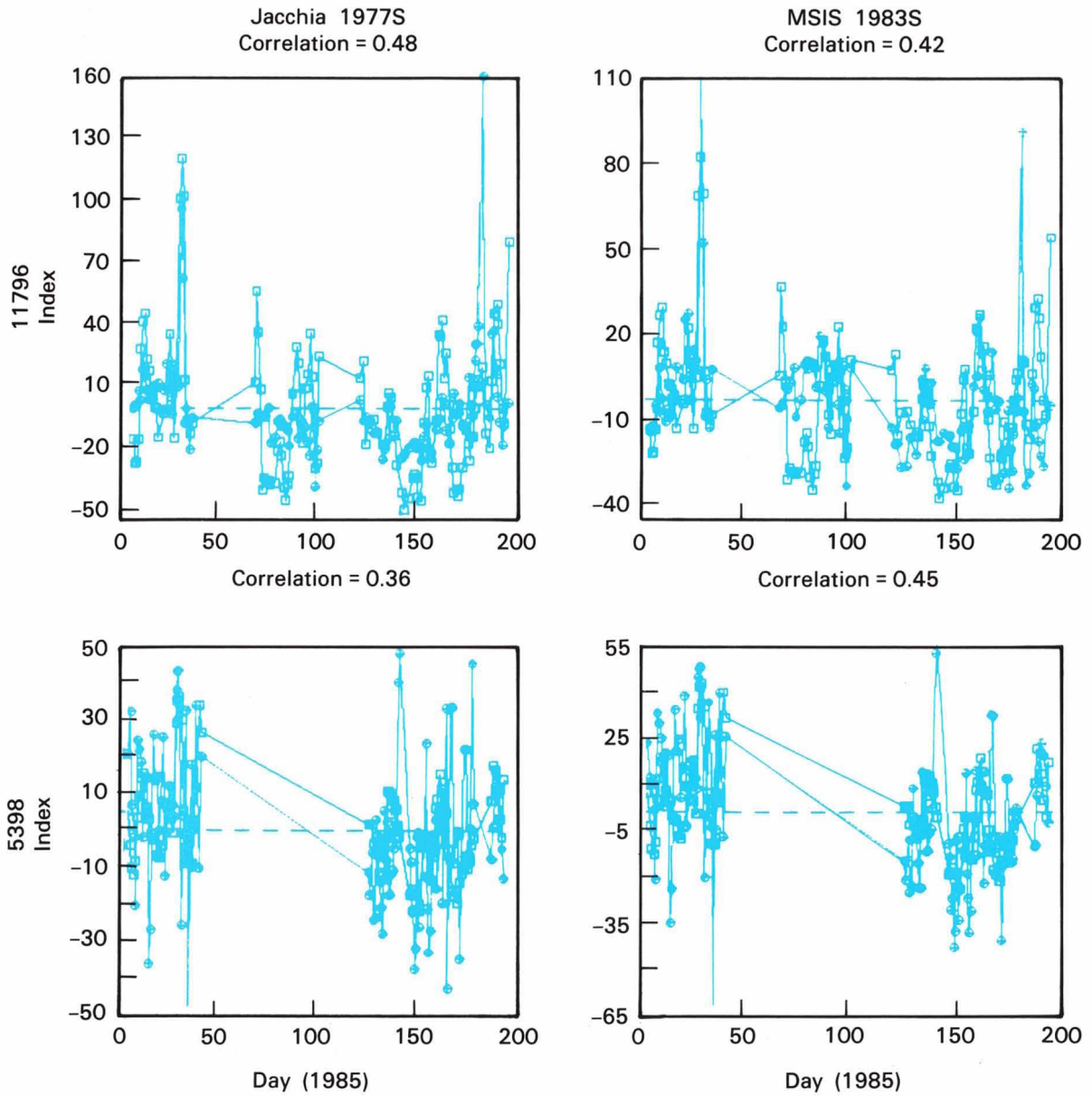


Fig. 8 — Correlation of precipitation index with scale factors.

the model differences exceeds 16%.

6. The J71 continues to perform exceptionally well and is the fastest overall. The MSIS83 is, by a large factor, the slowest.
7. For our overall use, balancing accuracy, computer speed, and range of height, we use the J77".
8. Satellite drag data plays an important role in understanding the thermosphere,

and in contributing unique data to monitor the next solar cycle.

Acknowledgments

We would like to acknowledge the individuals who made this data available to us through the radar tracking support provided by the Altair and Millstone radars. This work was sponsored by the Department of the Air Force.

References

1. L.G. Jacchia, "Atmospheric Models in the Region from 110 to 2000 km," in *COSPAR International Reference Atmosphere 1972*, International Council of Scientific Unions (Akademie-Verlag, Berlin, 1972), pg 227.
2. L.G. Jacchia, "Thermospheric Temperature, Density, and Composition: New Models," *S.A.O. Special Report No. 375* (Smithsonian Astrophysical Observatory, Cambridge, MA, 1977).
3. F. Barlier, C. Berger, J.L. Falin, G. Kockarts, and G. Thuillier, "A Thermospheric Model Based on Satellite Drag Data," *Ann. Geophys.* **34**, 9 (1978).
4. A.E. Hedin, "A Revised Thermospheric Model Based on Mass Spectrometer and Incoherent Scatter Data: MSIS-83," *J. Geophys. Res. A* **88**, 10,170 (1983).
5. G.E. Cook, "Satellite Drag Coefficients," *Planet. Space Sci.* **13**, 929 (1965).
6. F.A. Herrero, "The Drag Coefficient of Cylindrical Spacecraft in Orbit at Altitudes Greater Than 150 km," *NASA, Technical Memorandum 85043* (Goddard Space Flight Center, Greenbelt, MD, 1983).
7. E.M. Gaposchkin and A.J. Coster, "Evaluation of Recent Atmospheric Density Models," *Adv. Space Res.* **6**, 157 (1986).
8. A.E. Hedin, J.E. Salah, J.V. Evans, C.A. Reber, G.P. Newton, N.W. Spencer, C. Kayser, D. Alcayd, P. Bauer, L. Cogger, and J.P. McClure, "A Global Thermospheric Model Based on Mass Spectrometer and Incoherent Scatter Data: MSIS 1; N_2 Density and Temperature," *J. Geophys. Res.* **82**, 2139 (1977).
9. A.E. Hedin, C.H. Reber, G.P. Newton, N.W. Spencer, H.C. Brinton, and H.G. Mayr, "A Global Thermospheric Model Based on Mass Spectrometer and Incoherent Scatter Data, MSIS 2, Composition," *J. Geophys. Res.* **82**, 2148 (1977).
10. L.G. Jacchia and J.W. Slowey, "Analysis of Data for the Development of Density and Composition Models of the Upper Atmosphere," *AFGL-TR-81-0230* (Air Force Geophysics Laboratory, Hanscom Air Force Base, MA, 1981), AD-A-100420.
11. J.N. Bass, "Analytic Representation of the Jacchia 1977 Model Atmosphere," *AFGL-TR-80-0037* (Air Force Geophysics Laboratory, Hanscom Air Force Base, MA, 1980), AD-A-085781.
12. J.N. Bass, "Condensed Storage of Diffusion Equation Solutions for Atmospheric Density Model Computations," *AFGL-TR-80-0038* (Air Force Geophysics Laboratory, Hanscom Air Force Base, MA, 1980), AD-A-086863.
13. J.F. Liu, R.G. France, and H.B. Wackernagel, "An Analysis of the Use of Empirical Atmospheric Density Models in Orbital Mechanics, Spacetrack Report No. 4," Space Command, U.S. Air Force (Peterson Air Force Base, CO, 1983).
14. G. Afonso, F. Barlier, C. Berger, F. Mignard, and J.J. Walch, "Reassessment of the Charge and Neutral Drag of Lageos and Its Geophysical Implications," *J. Geophys. Res. B* **90**, 9381 (1983).
15. E.M. Gaposchkin, "Metric Calibration of the Millstone Hill L-Band Radar," *T.R. 721* (MIT Lincoln Laboratory, Lexington, MA, 1985), AD-A-160362.
16. E.M. Gaposchkin, "Calibration of the Kwajalein Radars," *T.R. 748* (MIT Lincoln Laboratory, Lexington, MA, 1986), AD-B-104457.
17. E.M. Gaposchkin, R.M. Byers, and G. Conant, "Deep Space Network Calibration 1985," *STK-144* (MIT Lincoln Laboratory, Lexington, MA, 1986).
18. E.M. Gaposchkin, L.E. Kurtz, and A.J. Coster, "Matera Laser Collocation Experiment," *T.R. 780* (MIT Lincoln Laboratory, Lexington, MA, 1987).
19. G.H. Kaplan (ed.), "The IAU Resolutions of Astronomical Constants, Time Scales and the Fundamental Reference Frame," *Naval Observatory Circular No. 163* (Naval Observatory, Washington, DC, 1981).
20. F.J. Lerch, S.M. Kloski, and G.P. Patel, "A Refined Gravity Model from Lageos" (GEM-L2), *Geophys. Res. Letters* **9**, 1263 (1982).
21. E.W. Schwiderski, "Global Ocean Tides, Part 1, A Detailed Hydrodynamical Model," *Rep TR-3866* (U.S. Naval Surface Weapons Center, Dahlgren, VA, 1978).
22. *Solar-Geophysical Data* (U.S. Dept. of Commerce, Boulder, CO, 1985).
23. J.C. Foster, J.M. Holt, R.G. Musgrove, and D.S. Evans, "Ionospheric Convection Associated with Discrete Levels of Particle Precipitation," *Geophys. Res. Let.* **13**, 656 (1986).
24. S.H. Gross, "Global Large Scale Structures in the F Region," *J. Geophys. Res. A* **90**, 553 (1985).



EDWARD MICHAEL GAPOSCHKIN is a senior staff member in the Surveillance Techniques Group. He has received a BSEE from Tufts University, a Diploma in numerical analysis from Cambridge University, and a PhD in geology from Harvard

University. Mike's work at Lincoln Laboratory has been centered on problems in satellite surveillance; his efforts have enabled Lincoln's Millstone radar to produce data of geodetic quality. Before joining Lincoln Laboratory, Mike spent 22 years with the Smithsonian Astrophysical Observatory. He is the author of over 100 journal articles in the fields of satellite geodesy, metric orbit analysis, and radar metric data improvements.



ANTHEA J. COSTER is a staff member in the Surveillance Techniques Group, where she concentrates on studies of the atmosphere. She conducts her research at Lincoln's Millstone radar site in Westford, Mass. She re-

ceived a BA degree from the University of Texas in mathematics and an MS and a PhD degree from Rice University in space physics and astronomy. Before joining Lincoln Laboratory, Anthea worked for the Radar and Instrumentation Laboratory of the Georgia Tech Research Institute.